Microfocus X-ray Sources for Short Wavelength Radiation

Bernd Hasse[1], Jürgen Graf[1], Francesca P. A. Fabbiani[2], Mike R. Probert[3], Andres E. Goeta[3], Judith A. K. Howard[3], Carsten Michaelsen[1]

[1] *Incoatec GmbH, Max-Planck-Str. 2, 21502 Geesthacht, Germany*
[2] *Geowissenschaftliches Zentrum, Universität Göttingen, Goldschmidtstr. 1, 37077 Göttingen, Germany*
[3] *Chemistry Department, Durham University, South Road, Durham, DH1 3LE, United Kingdom*

Introduction

In a high-pressure X-ray diffraction experiment using a diamond anvil cell (DAC), the area of reciprocal space accessible during data collection is primarily restricted by the geometry of the DAC. For a typical experiment using Mo radiation, only a small fraction of all reflections can be collected. This can be as low as 30 % for triclinic crystal structures. Using radiation with a shorter wavelength, such as Ag-Kα, a larger portion of the reciprocal space is accessible, thus increasing the number of observations and the completeness of the data. However, conventional Ag sealed tube sources are rarely used for high-pressure studies because of their low intensity.

Microfocus sealed tube sources, such as the Incoatec Microfocus Source (IμS), have proven to deliver flux densities beyond that of traditional X-ray sources when combined with 2D focusing multilayer mirrors [1, 2]. This type of sources presents a promising alternative to classical sealed tube sources currently being used in high-pressure crystallography.

Beam Characteristics of the IμS

The Ag-IμS delivers a focused and monochromatic X-ray beam with a FWHM of 0.09 mm in the image focus. In contrast to the typical top-hat shaped beam profile that is produced by sources coupled to a flat graphite monochromator, the beam profile from the IμS has a symmetrical Gaussian-shaped intensity distribution. As a consequence, the flux density increases with decreasing sample size (Fig. 1), thus leading to strong diffracted intensities especially for small samples. Furthermore, the convergent beam from the IμS reduces the background of the data by minimizing the scattering from peripherals, such as conventional crystal mounts or gaskets. The integrated intensity of the original Ag-IμS, which is available since 2009, is at least about three times higher than the intensity of a 1.5 kW Ag sealed tube system. The new Ag-IμS$^{\text{High Brilliance}}$ has an improved X-ray optical design that results in a further intensity gain of 50% when compared to the original Ag-IμS.

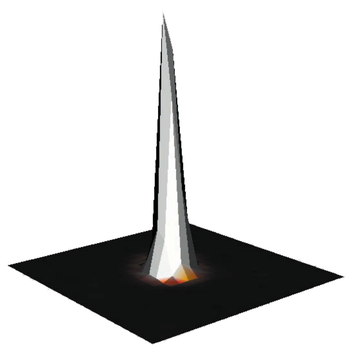

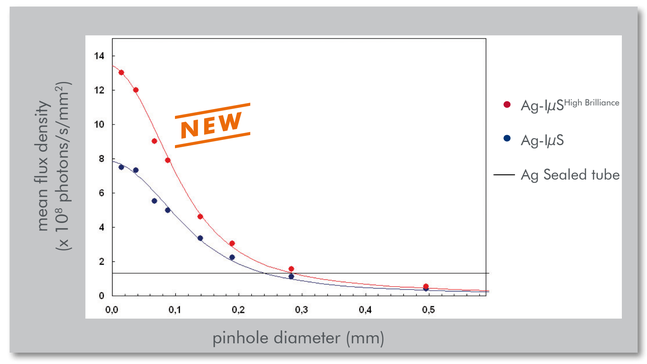

Fig. 1: Gaussian-like beam profile of the Ag-IμS (left, FWHM = 0.09 mm, 5 mrad divergence); Comparison of the flux density measured with a calibrated PN diode (right).

Performance Comparison of Ag-IμS vs. 2 kW Mo Sealed Tube

Comparative measurements have been performed on a Bruker AXS APEX II goniometer using the original Ag-IμS and a 2 kW Mo sealed tube, which was equipped with a flat graphite monochromator and a modified 0.5 mm collimator. The beam from the multilayer mirror of the Ag-IμS was focused on the sample position. A crystal of gabapentin heptahydrate in a Be-free DAC was applied for both data collections using comparable data collection strategies.

Source	Ag-IμS	Mo-ST
Power [kW]	0.03	2.0
Exposure time [s/0.3°]	20	20
<*I*>	368.8 (64.9)*	378.0 (61.0)*
<*I*/σ>	19.6 (3.2)*	18.3. (4.7)*
Unique data	866 (170)*	721 (135)*
<Complete.> [%]	40.6 (28.9)*	33.7 (22.6)*
<Redundancy>	1.5 (0.9)*	1.1 (0.7)*
R(int) [%]	3.06 (16.36)*	3.42 (14.89)*
*R*1 (*I*>2σ(*I*))$^{\#}$ [%]	4.87 (630)$^{\#}$	5.32 (523)$^{\#}$
*wR*2 (all)$^{\&}$ [%]	10.25 (860)$^{\&}$	12.32 (705)$^{\&}$

Tab. 1: Data statistics for the comparative measurement on Gabapentin heptahydrate (max. resolution 0.90 Å (1.00 – 0.90 Å); $^{\#,\&}$ number of unique reflections used).*

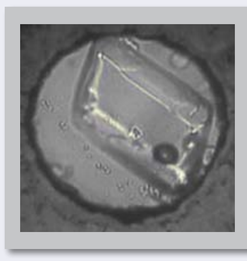

Fig. 2: Gabapentin heptahydrate crystal ($C_9H_{17}NO_2 \cdot 7H_20$; P-1) in a 0.3 mm inconel gasket at 0.8 GPa [3].

Due to the shorter wavelength of Ag (0.56 Å) compared to Mo (0.71 Å) radiation, a larger section of the reciprocal space is recorded per image when using the same detector distance (Fig. 3). As a consequence, Ag-IμS data have significantly higher completeness than data recorded with Mo radiation. Thus, the Ag-IμS data set of gabapentin contains about 20% more unique reflection and has a higher redundancy (Tab. 1). The Ag-IμS has a higher flux density than a Mo sealed tube. Furthermore, the small cross-section of the convergent beam significantly reduces the background that results from scattering at the gasket of the DAC (Fig. 3). The overall integrated intensity and the signal-to-noise ratio of the Ag-IμS data are, therefore, higher compared to the Mo sealed tube data. The results from the structure refinement clearly underline the predominance of the Ag-IμS data set.

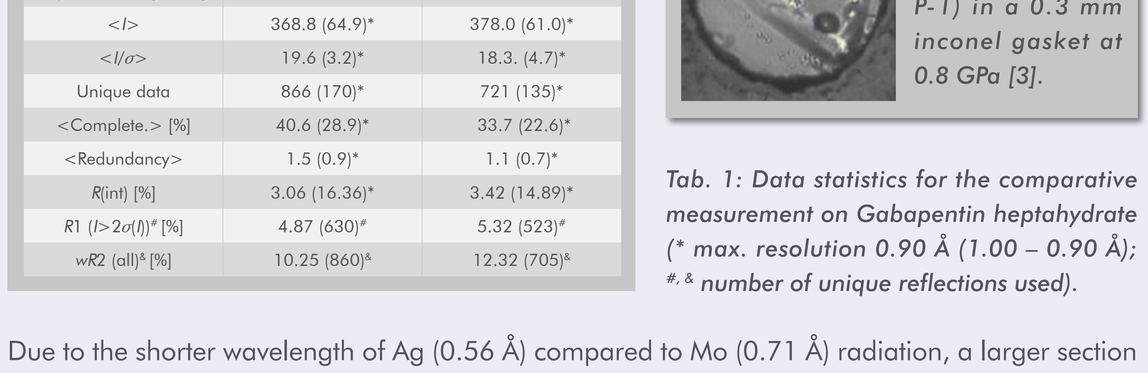

Fig. 3: Diffraction patterns of the Gabapentin crystal: Original Ag-IμS (left); 2 kW Mo sealed tube (middle); Illustration of the gain in completeness with Ag radiation (right, original Ag-IμS).

High-Pressure Study on Cytidine

As a case study of a phase transition under high-pressure, the crystal structure of Cytidine ($C_9H_{13}N_3O_5$) was determined at ambient pressure and at pressures of 0.82 GPa, 1.98 GPa and 2.56 GPa. Furthermore, the low temperature structure was determined at 2 K. The data was collected using a small single crystal of Cytidine (0.23 x 0.08 x 0.07 mm^3) that was mounted on a Huber 4-circle diffractometer equipped with an Apex II detector. For the high-pressure experiments, an original Ag-IμS was used, while for the room and low temperature structure a Mo-TXS microfocus rotating anode was used [4]. The crystal structures of the high-pressure phases have been solved using SHELXD [5].

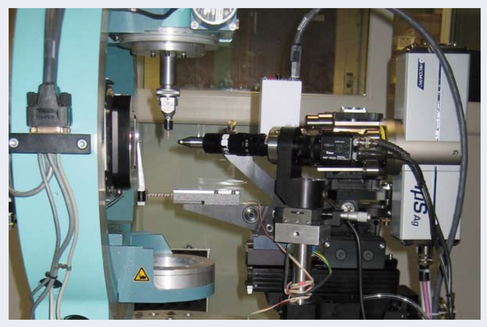

Fig. 4: Ag-IμS mounted on a Huber 4-circle diffractometer.

Source	Mo-TXS	Mo-TXS	Ag-IμS
Conditions	290 K, 1 atm	2 K, 1 atm	290 K, 2.56 GPa
Exposure time [s/0.5°]	20	20	30
Max. Resolution [Å]	0.72	0.72	0.80
<*I*/σ>	11.0 (1.2)	23.4 (5.2)	27.7 (2.9)
Resolution [Å]	9.00 - 0.83 (0.93 - 0.83)		
<*I*/σ>	15.5 (2.2)	36.0 (11.1)	30.0 (4.1)
Unique data	947 (294)	1043 (296)	849 (208)
<Complete.> [%]	80.5 (93.3)	90.0 (94.3)	44.7 (39.5)
<Redundancy>	3.7 (2.6)	7.1 (5.3)	6.2 (2.7)
R(int) [%]	5.73 (31.40)	4.90 (14.42)	5.61 (37.71)
R(σ) [%]	5.85 (45.96)	2.93 (11.43)	3.91 (32.18)
*R*1 (*I*>2σ(*I*))$^{\#}$ [%]	6.99 (1131)$^{\#}$	4.52 (1923)$^{\#}$	5.00 (1177)$^{\#}$
*wR*2 (all)$^{\&}$ [%]	11.06 (2282)$^{\&}$	8.89 (2456)$^{\&}$	12.49 (1670)$^{\&}$

Tab. 2: Data statistics for the room temperature and low temperature crystal structure of Cytidine ($P2_12_12_1$, 157 parameters) and for the crystal structure at 2.56 GPa ($P2_1$, 143 parameters and 45 restraints, $^{\#,\&}$ number of unique reflections used).

While the crystal structure of Cytidine is orthorhombic with the space group $P2_12_12_1$ at room temperature and at 2 K, a phase transition from orthorhombic to monoclinic occurs at high pressure. With increasing pressure, the angle β is continuously increasing from 90.1° at 0.82 GPa to 90.8° at 2.56 GPa resulting in the space group $P2_1$ which is a maximal translation equivalent subgroup index 2 (t2) of $P2_12_12_1$. A further increase in the pressure results in a catastrophic degradation of the sample above 2.70 GPa. The loss of symmetry by the shift of the angle β changes Z′ from being Z′ = 1 for the room and low temperature structure to Z′ = 2 for the structure of the high-pressure phases.

Conclusion

The Ag-IμS is a powerful X-ray source for high-pressure crystallography that outperforms classical sealed tube sources. The high flux density and the reduced background lead to high integrated intensities. The new Ag-IμS$^{\text{High Brilliance}}$ delivers even 50% more intensity compared to the original Ag-IμS. The higher resolution and number of unique data, as well as the higher redundancy facilitate structure solution and refinement of high-pressure phases.

Acknowledgement

We thank S. Parsons (University of Edinburgh) for a copy of the program ECLIPSE [6].

References

[1] T. Schulz, K. Meindl, D. Leusser, D. Stern, J. Graf, C. Michaelsen, M. Ruf, G.M. Sheldrick, D. Stalke, *J. Appl. Cryst.* **2009**, 42, 885.

[2] J. Wiesmann, J. Graf, C. Hoffmann, A. Hembd, C. Michaelsen, N. Yang, H. Cordes, B. He, U. Preckwinkel, K. Erlacher, *Particle & Particle Systems Characterization* **2009**, 26, 112.

[3] F.P.A. Fabbiani, D.C. Levendis, G. Buth, W.F. Kuhs, N. Shankland, H. Sowa, *CrystEngComm.* **2010**, 12, 2354.

[4] M.R. Probert, C.M. Robertson, J.A. Coome, J.A.K. Howard, B. Michell, A.E. Goeta, J. *Appl. Cryst.* **2010**, 43, 1415.

[5] G.M. Sheldrick, *Acta Cryst.* **2008**, A64, 112.

[6] A. Dawson, D.R. Allan, S. Parsons, M. Ruf, *J. Appl. Cryst.* **2004**, 37, 410.